DYNAMIC COMPRESSION OF POROUS METALS AND THE EQUATION OF STATE WITH VARIABLE SPECIFIC HEAT AT HIGH TEMPERATURES

S. B. KORMER, A. I. FUNTIKOV, V. D. URLIN, and A. N. KOLESNIKOVA

Submitted to JETP editor August 10, 1961

J. Exptl. Theoret. Phys. (U.S.S.R.) **42**, 686-702 (March, 1962)

Results of an investigation of dynamic compression of Al, Cu, Pb and Ni are presented for various initial densities and pressures between 0.7 and 9×10^{12} dyn/cm^2. The laws of shock compression of porous substances are studied. A new form of the equation of state is presented, which allows for the decrease of the specific heat and of the Grüneisen coefficient with increasing temperature. The parameters of the equation are determined for four of the investigated metals. Values of the "electron" analog of the Grüneisen coefficient are determined for Cu and Ni and its magnitude is estimated for Pb and Al.

INTRODUCTION

STUDY of the dynamic compression of many metals [1-5] has yielded for them an equation of state which is valid, strictly speaking, only for the shock compression adiabat and the "cold" compression isotherm $P_c(\rho)$ at T = 0°K. In this region, atomic elastic interaction forces predominate and no functional equations can be deduced to relate the thermal factors with the temperature or the density ρ. It was thus shown, for example, [6] that the same experimental data, especially at relatively low compressions $\sigma = \rho/\rho_0 \leq 1.5$, can be described by essentially different dependences of the Grüneisen coefficient γ on the density with nearly equal values of $P_c(\rho)$.

Zel'dovich [7] proposed to investigate shock compression of matter in which the initial density has been decreased below normal. Such investigations yield much more complete information on the thermodynamic properties of matter at high pressures and temperatures. In porous matter individual particles of solid matter of normal density ρ_0 are separated by empty spaces so that its average density is $\rho_{00} = \rho_0/m$, where m is the degree of porosity. In adiabatic compression the work done by the external pressure is first consumed in closing the pores and is connected with overcoming the friction forces between the particles and their deformations. A shock wave of even low intensity compresses porous matter to the density of the solid matter, so that all that needed be overcome is the strength of the material, the order of magnitude of which is 10^9 dyn/cm^2 and decreases with heating of the substance. Consequently, for pressures on the order of 10^{12} dyn/cm^2,

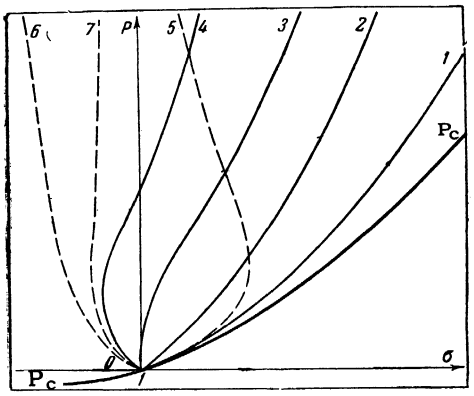

FIG. 1. Dynamic adiabats of substances of different porosities; continuous lines – adiabats of the first type [$g < 2/(m\sigma - 1)$], dashed – adiabats of the second kind [$g > 2/(m\sigma - 1)$].

the point (1,0) on Fig. 1 will be, with high degree of accuracy, a common point for the shock-compression adiabats of the solid and porous substances. As we vary ρ_{00}, the experimental points will fill the entire P-ρ field between the dynamic adiabat of the solid substance (adiabat 1 of Fig. 1) and the ordinate $\sigma = 1$ (adiabats 2 and 3 of Fig. 1).

When the porosity is high, the role of heat may prove to be so important that, as shown by Zel'dovich and Kompaneets with the Mie-Grüneisen equation of state as an example and by Zababakhin for an arbitrary equation of state, the pressure increase in the shock wave leads to a decrease in density, i.e., $(\partial P/\partial\sigma)_H$ becomes negative (adiabat 6 of Fig. 1). This conclusion follows from the relation

$$\left(\frac{\partial P}{\partial \sigma}\right)_H = \left\{\left(\frac{\partial P}{\partial \sigma}\right)_T + \rho_0\sigma^2\left(\frac{\partial P}{\partial E}\right)_\sigma\left[T\left(\frac{\partial P}{\partial T}\right)_\sigma - \frac{P_H}{2}\right]\right\} \Big/ \left[1 - \frac{m\sigma - 1}{2\rho_0\sigma}\left(\frac{\partial P}{\partial E}\right)_\sigma\right], \quad (1)$$

which can be obtained (see, for example, [8]) from the thermodynamic identity $dE = TdS - PdV$ and the Hugoniot adiabat of porous matter in the form

$$\Delta E_H = (m\sigma - 1) P_H / 2\rho. \quad (2)$$

If we use as an example an equation of state with electronic components [4,6]:

$$P = P_c + 3R\rho\gamma(T - \hat{T}) + \tfrac{1}{2} g\beta\rho T^2, \quad (3)$$

$$E = E_c + 3R(T - \hat{T}) + \tfrac{1}{2}\beta T^2, \qquad E_c = \int_{\rho_k}^{\rho} P_c\, d\rho / \rho^2 \quad (4)$$

[where R is the gas constant,

$$\hat{T} = T_0 - E_0/3R, \qquad E_0 = \int_0^{T_0} C_v\, dT,$$

E_0—internal energy under normal conditions ($P = 0$, $T = T_0 = 300°K$), C_V—the Debye specific heat, β—the coefficient of electronic specific heat, $g = (d \ln \beta)/(d \ln \rho)$, and ρ_k—density at $P = 0$ and $T = 0°K$] we can readily deduce from (1) that adiabats can exist in which sections having positive and negative values of $(\partial P/\partial\sigma)_H$ alternate. The reversal in the sign of $(\partial P/\partial\sigma)_H$ is physically explained by the fact that at small pressures and temperatures the character of the function $P_H(\sigma)$ is governed by the behavior of the lattice, while at large pressures it depends on the behavior of the electrons. In other words, the sign of $(\partial P/\partial\sigma)_H$ is determined by the relation between γ, g, and $m\sigma$.

When $g < 2/(m\sigma - 1) = P_H/\rho\Delta E_H$, the derivative $(\partial P/\partial\sigma)_H$ is positive, does not reverse sign in the region $\sigma > 1$ (adiabats 1, 2, and 3 of Fig. 1), and has alternating signs in the region $\sigma < 1$ (adiabat 4 of Fig. 1). We call these adiabats of the first type. An adiabat similar to 2 was obtained by Al'tshuler, Krupnikov, and Ledenev [2] for porous iron, while an adiabat similar to 4 was obtained by Krupnikov and Brazhnik for porous tungsten. When $g > P_H/\rho\Delta E_H$ the situation reverses. The adiabats are similar to curves 5 and 6 of Fig. 1 and are called adiabats of the second type. The values of P_H and σ for which $(\partial P/\partial\sigma)_H = \infty$, are determined by certain combinations of γ, g, P_c, and $m\sigma$. When $\sigma > 1$, γ and g cannot be simultaneously larger than $P_H/\rho\Delta E_H$, and when $\sigma < 1$ they cannot be simultaneously smaller than this quantity. The density limit is reached when $g = 2/(m\sigma - 1)$ (adiabat 7 on Fig. 1). Finally, the shock adiabat can have a point of inflection if the $g(\sigma)$ curve crosses the hyperbola $f(\sigma) = 2/(m\sigma - 1)$ twice.

Thus, the very shape of the adiabat allows us to determine the limiting values of the electronic analog of the Grüneisen coefficient g, which heretofore could not be measured under static conditions. Analysis of the experimental data on shock compression of porous metals, within the framework of the chosen equation of state, yields (see Sec. 4) not only the limit of g, but its exact value.

The substance behind the front of a powerful shock wave traveling through a highly porous metal is undoubtedly in the liquid or even gaseous state (dense gas of strongly interacting atoms). It is sufficient to state that the temperatures attained on the dynamic adiabat of nonporous aluminum at $P_H \sim 2 \times 10^{12}$ dyn/cm^2 or copper and lead at $P_H \sim 4 \times 10^{12}$ dyn/cm^2 are estimated [4] to be approximately double the melting temperatures at these pressures. Shock compression of porous metals is accompanied by much greater heating.[2] It is therefore necessary to allow for the temperature variation of the specific heat of the lattice, from the value 3R characteristic of a solid at temperatures on the order of several times Θ (the Debye temperature), to the value 3R/2 characteristic of a liquid that approaches the gaseous state.[9] For a given density, the ratio $\lambda_l = P_{Tl}/\rho E_{Tl}$ of the thermal pressure due to lattice atom vibrations (P_{Tl}) to the density of its thermal energy (ρE_{Tl}) should change with increasing temperature from the value of γ corresponding to the given density at $T \sim 0°K$ to the value $\frac{2}{3}$ corresponding to $T \to \infty$.

Considering the accuracy of the experiment, it is impossible to determine these temperature dependences by investigating shock compression of metals of normal initial density, for at practically attainable pressures, the temperature on the shock adiabat increases with increasing density almost as fast as the slope of the curve of "cold" or elastic compression $c_c^2 = dP_c/d\rho$. As will be shown in Sec. 3, the ratio $z = lRT/c_c^2$ (where l is constant for a given substance) determines the measure of deviation from the laws that govern solids. Shock compression of porous substances has made it possible to create states with high temperatures at low compressions, where c_c is relatively small, and thereby obtain the necessary experimental material for solving the problem formulated above.

A systematic investigation of three simple metals (aluminum, copper, and lead) and one transition metal (nickel) of varying porosity ($m = 1$—4) enabled us to obtain shock-compression adiabats with σ ranging from 0.9 to 2.2 and P_H ranging from 0.7×10^{12} to 9×10^{12} dyn/cm^2.

The most thoroughly investigated were copper and nickel.

We present in this paper a semi-empirical interpolation equation of state, which accounts for the temperature and density variations of the specific heat and the Grüneisen coefficient. The form obtained for the equation of state is suitable for a description of the thermodynamic state of metals in the region where the solid and the gaseous phases exist. The validity of the chosen form is confirmed by the satisfactory agreement between the experimental data and the calculated shock adiabats of metals with different initial porosity. The value of the electronic analog of the Grüneisen coefficient is found for copper and nickel and is estimated for lead and aluminum.

1. INVESTIGATED SUBSTANCES. PROCEDURE AND EXPERIMENTAL RESULTS

The investigated specimen was a metal powder compressed to an average density ρ_{00}. The fine grains were separated from commercial powder with a type FR-1 sieve, followed by further air cyclone separation. The grain size was determined in a PSKh-2 instrument [10] from the specific surface area and checked with a microscope. Careful attention to grain dimension was necessary because the front of a shock wave produced by relaxation in a porous substance has an estimated width of the same order of magnitude as the grain. The characteristics of the powders used in the investigation are listed in Table I. Special experiments have established that at pressures $(0.1-0.2) \times 10^{12}$ dyn/cm^2 in porous copper ($m = 4$) and 0.3×10^{12} dyn/cm^2 for porous lead ($m = 1.67$) a change in dimensions of individual grains ranging from 0.5 to 100 μ does not affect the velocity of the shock wave. This should influence the results of the measurements even less in the pressure range investigated by us.

Table I

Metal	Brand of powder	Content of original metal, %	Average dimension of selected grains	Loose-powder porosity
Al	PAK-3	92,5	1	6
Cu	PM-2	99,7	5	4
Pb	SO	99,5	19	1.7
Ni	—	99,5	8	3

Specimens of average density were produced at low pressures (up to 20 kg/cm^2), while higher porosity (lower density) was obtained by filling thin-wall cylindrical boxes with metallic powder. The maximum porosity of the investigated metals corresponded to a density somewhat greater than that of loose powder. The relation $\Delta m/m \leq 1$ was maintained within each series of experiments. The parameters of the shock waves in porous metals were determined by the reflection [1,3] and deceleration [2] methods.

In the reflection method (the first group of experiments), a shock wave was produced in an iron shield by impact with an iron plate accelerated by explosion products to a velocity $W = 8.64$ km/sec. This striker velocity in the screen corresponds to $P_H = 356.8 \times 10^{10}$ dyn/cm^2, $\sigma = 1.664$, shock-wave velocity $D = 10.67$ km/sec, and mass velocity $U = 4.26$ km/sec. In the deceleration method, i.e., collision between a flying plate and the investigated substance (second group of experiments), the iron shock driver was also accelerated by explosion products. The rate of collision amounted to 15.45 km/sec.* In the processing of the experimental results we used the dynamic adiabat given for iron in [4], extrapolated to the pressure region $\sim 10^{13}$ dyn/cm^2 using the data of Al'tshuler, Bakanova, and Trunin. We took account here of the damping of the shock wave, as was done in [4], and for the heating of the shock driver during acceleration.

The measurements were made on cylindrical specimens 6—10 mm high; the diameter and height were chosen such as to prevent the shock wave from being affected by disturbances propagating from the lateral surface.[11] The propagation time of the shock wave through the specimen was measured with OK-21 oscillographs which registered signals from electric contact-making transmitters.[2] The velocity of the shock wave was determined in a series of 4—8 experiments, each consisting of 4—6 readings. From among the 15—45 measurements we eliminated those deviating from the mean by more than allowed for by the criterion for the statistical data reduction.†

The wave velocities of the four investigated metals, measured in specimens of different poros-

*A similar measuring device was used earlier by Al'tshuler, Krupnikov, and Ledenev to measure the compressibility of iron at 10^{13} dyn/cm^2. The apparatus developed by the authors differed principally in that a thicker shock drive was used to eliminate the influence of the overtaking relaxation[11] in specimens of porous metal.

†A reading was discarded if the probability of such deviations or of even greater deviations from the mean value, obtained for the normal distribution, does not exceed 1/n, where n is the total number of measurements. This criterion is somewhat more stringent than the Chauvenet criterion.[12]

Table II

Metal	First group of experiments				Second group of experiments			
	Porosity,	D, km/sec	$P_H \times 10^{-12}$, dyn/cm²	σ	Porosity	D, km/sec	$P_H \times 10^{-12}$ dyn/cm²	σ
Al	1.43	11.74±0.10	1.391	1.498	1.00	18.31±0.16	4.93	2.185
	2.08	11.42±0.09	1.003	1.176				
	2.98	10.75±0.08	0.702	1.015				
Cu	1.57	9.22±0.04	2.626	1.395	1.00	14.78±0.16	9.55	1.960
	2.00	9.15±0.07	2.204	1.219	1.57	14.32±0.34	7.01	1.595
	3.01	8.85±0.07	1.582	1.045	2.00	14.39±0.12	5.95	1.402
	4.00	8.79±0.03	1.260	0.927	4.00	14.50±0.14	3.54	1.018
Pb	1.67	7.79±0.04	2.642	1.670	1.67	12.74±0.16	7.30	1.774
Ni	1.43	9.79±0.26	2.908	1.364	1.00	14.87±0.20	9.56	1.946
	1.75	9.42±0.18	2.469	1.261	1.75	15.55±0.27	6.87	1.295
	3.00	9.25±0.15	1.639	0.941	3.00	15.58±0.27	4.67	0.949

ity, are listed in Table II (the notation was given above) together with other parameters of the experimental points. The wave velocities are given with the rms mean-value errors used as a measure of the accuracy.

The wave velocities obtained for each metal, under equal-charge conditions, are shown as functions of m in Fig. 2, where they are combined into "equal-charge lines" of constant shock-wave parameters in the screen (reflection method) or of constant collision velocity (deceleration method).

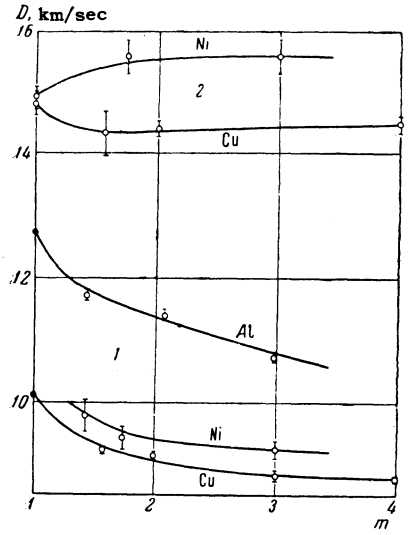

FIG. 2. Dependence of the wave velocities on m, obtained under conditions of equal charge, for two different values of the charge (1 and 2); o – data of present work (with possible errors indicated), ● – from[4].

The functions D(m) yield sufficiently reliable values of the wave velocity in a metal of any intermediate porosity, and allow the points on the Hugoniot adiabat to be determined for all the investigated P_H-σ region. In P_H-σ coordinates, the experimental data and the "equal-charge lines" are plotted in Figs. 3–6. For each experimental point we indicate the scatter corresponding to ΔD/D of Table II. The relative error in the pressure, $\Delta P_H/P_H = \Delta D/2D$, is smaller than the relative error in the velocity of the shock wave,* while the error in the degree of compression $\Delta\sigma/\sigma = (3/2)(m\sigma - 1)\Delta D/D$ is greater.

2. DISCUSSION OF EXPERIMENTAL RESULTS

From a qualitative examination of the experimental data it follows that all the adiabats of copper and aluminum, and at least some of the adiabats of nickel and lead, are of the first type. The majority have the same appearance as adiabats 1, 2, and 3 of Fig. 1. The adiabats Cu (m = 4) and Al (m = 3) have portions in which $(\partial P/\partial\sigma)_H$ is greater as well as less than zero (adiabat 4 of Fig. 1). The adiabat of porous nickel with m = 3 has a singular behavior, since nearly the same densities are attained for essentially different pressures (adiabat 7, Fig. 1). In other words, in the case of nickel, the density limit is already reached in the experimentally investigated pressure region,

$$\sigma_{\text{lim}} = m^{-1}(1 + 2/g). \qquad (5)$$

Let us see the extent to which the experimental data on shock compression of porous and solid metals are described by an equation of state with electronic components, using the already published data[6].† As can be seen from Figs. 3–6, the difference between the calculated adiabats (dashed lines) and the experimental ones at m = 1 does not exceed 8% in the entire range of investigated pressures. The newly obtained experimental points for aluminum at 4×10^{12} dyn/cm² and for copper

*The relations for $\Delta P_H/P_H$ and $\Delta\sigma/\sigma$ were obtained assuming that the adiabat of iron is reliably known.

†An equation of state with g = ½ was found for nickel, similar to that obtained in[6]. The reference point used was $P_H = 1.5 \times 10^{12}$ dyn/cm² and σ = 1.388.[5]

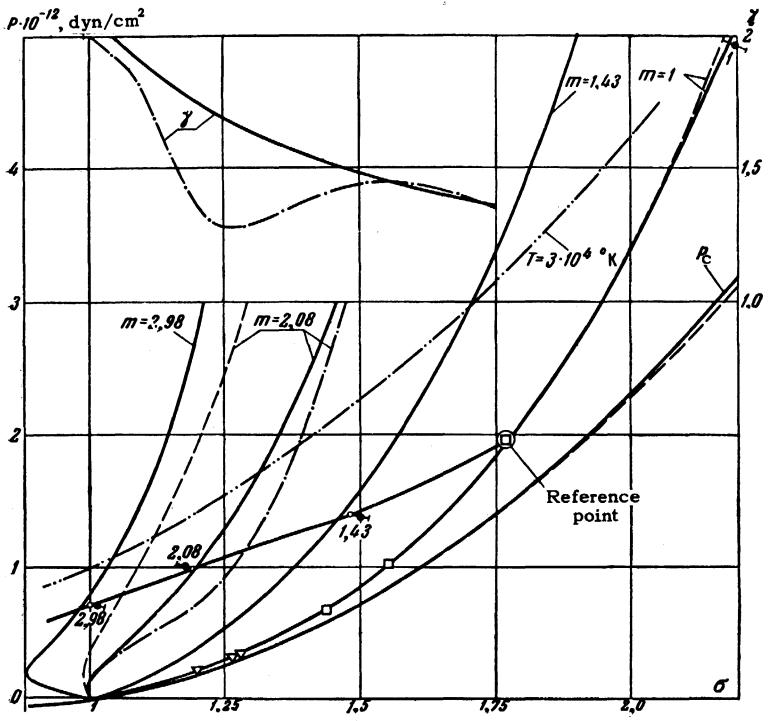

FIG. 3. Dynamic adiabats for aluminum of different porosity: ● – experimental points, ○ – averaged points from Fig. 2, ▽ – from [1], □ – from [4], △ – from [5]; continuous lines – calculated adiabats, dashed lines – from [6], dashed-dot lines from [4] with $l = 6$, double dash-dot line – isotherm.

at 9×10^{12} dyn/cm^2 have confirmed the correctness of the extrapolation undertaken for these metals in [6].* However, when $m \geq 1.5$ there is already a noticeable difference, which grows appreciably with increasing porosity, and when $m \geq 3$ the form of the calculated adiabat loses physical meaning. What is striking is the difference in the relationship between the calculated and experimental adiabats between the simple metals aluminum and copper and the transition metal nickel. Whereas the calculated adiabats for the first two metals (see, for example, the case with $m \sim 2$, dashed lines of Figs. 3 and 4) lie appreciably above the experimental points (beyond the limits of experimental error), the situation is reversed for nickel (for example, the calculated adiabat with $m = 3$, Fig. 6).

Since the elastic curves are determined from the dynamic adiabats with $m = 1$ with sufficient reliability, especially at low compressions, the reason for the observed discrepancies should be sought in the thermal components of the pressure and of the energy. For this purpose we examine the quantity $\lambda = (P - P_c)/\rho(E - E_c)$—the analog of the Grüneisen coefficient in the equation with the electronic components—which for known P_c and E_c [6] can be determined from experimental data alone. Fig. 7 shows $\lambda(\sigma)$ for copper, calculated along the "equal-charge lines" from the equation of state with electronic components (λ^t)

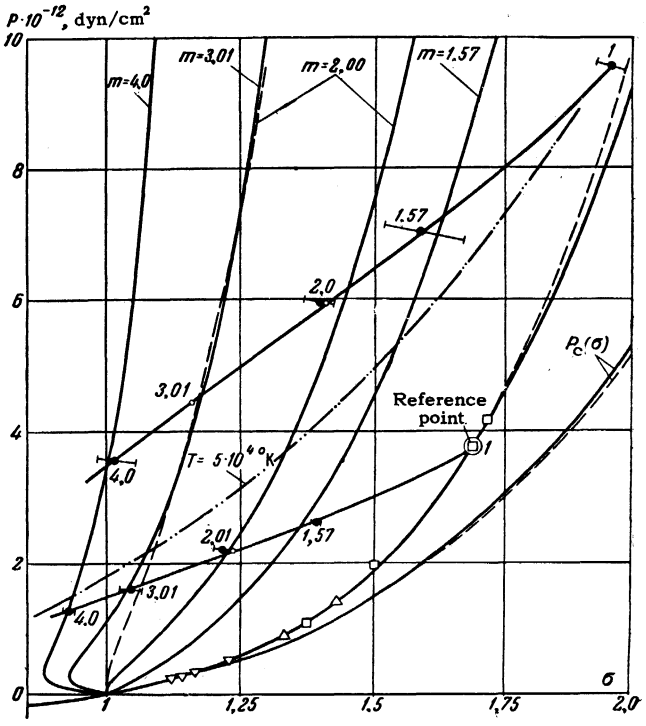

FIG. 4. The same as Fig. 3, but for copper (same notation).

*The experimental point for copper, obtained by Al'tshuler, Bakanova, and Trunin in this range of pressures, lies somewhat to the right (within the limits of the total experimental scatter) and is also close to the extrapolated adiabat. The reason for the difference between the two points is not clear. The results obtained for nickel, under the same conditions, practically coincided.

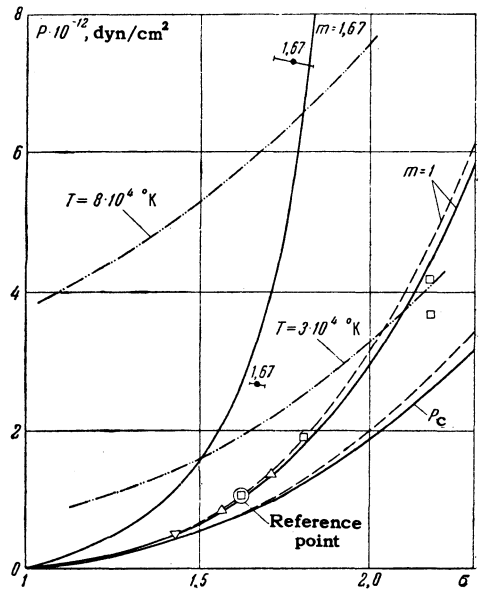

FIG. 5. The same as Fig. 3, but for lead (same notation).

and from the averaged experimental data (λ^e). Since $\lambda^e < \lambda^t$ at high temperatures, it follows (when $T^e < T^t$) that at least λ_l or $\bar{C}_V = E_{T_l}/T$ decrease with increasing temperature.* This can be readily verified from the relation

$$\lambda^t = \lambda_1\left[1 - \frac{1 - 1/2\,\lambda_1}{1 + 2\,\bar{C}_v}\right].$$

When $T^e > T^t$, an analogous conclusion can be drawn from the relation

$$3R\,(2\lambda^t - 1)\,T^t > (2\lambda_1 - 1)\,\bar{C}_v T^e,$$

which follows from (2) and (3). The same holds true for aluminum.

Thus, the experiment shows unambiguously that for simple metals the equation of state with electronic components must be made more precise at least by taking into account the decrease in the Grüneisen coefficient or in the specific heat of the lattice with increasing temperature. It is necessary to bear in mind here that one cannot use for transition metals the values of the electronic analog of the Grüneisen coefficient which follow from the calculations by the Thomas-Fermi model.† This conclusion follows from an analysis of the

*If λ_l is independent of the temperature, it is identically equal to γ in (3).

†The Thomas-Fermi statistical model of the atom cannot describe the atomic electron-structure details that distinguish transition metals from simple metals. This affects not only the value of g, but also the value of the coefficient of electronic specific heat, β. Whereas for simple metals the Thomas-Fermi model yields values of β that are close to those experimentally obtained at low temperatures, for transition metals the difference is appreciable.

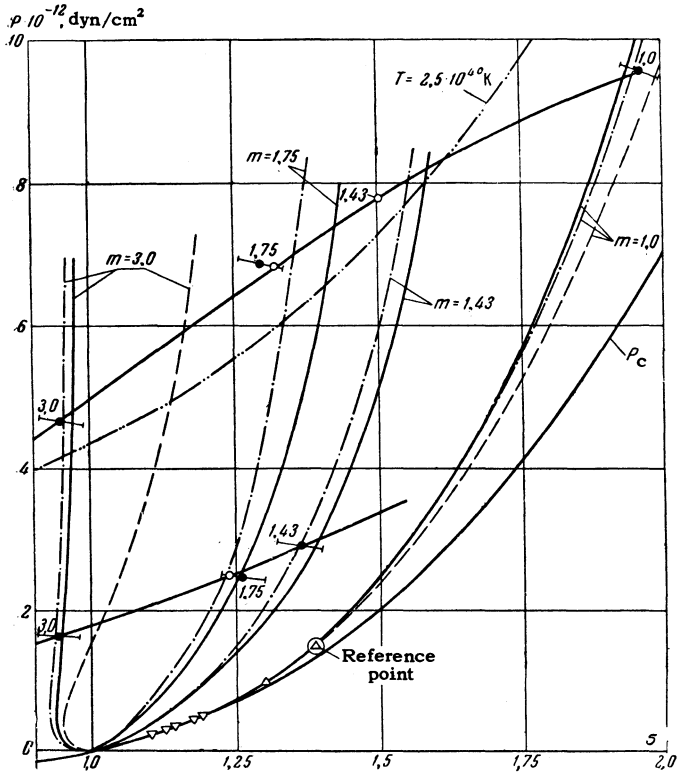

FIG. 6. The same as Fig. 3, but for nickel. Continuous lines – calculated adiabats with g = 1, dash-dot lines – with g = g (δ). For notation see Fig. 3.

experimental adiabat of nickel with m = 3, which can be reconciled only with a value g ~ 1, in place of the g ~ 0.5 that follows from the Thomas-Fermi model. This is also shown by the sign of the difference between the calculated and experimental adiabats of nickel with m = 1.75, since inclusion of the temperature dependence of λ_l and of C_V only aggravates the existing contradiction.

3. EQUATION OF STATE WITH ELECTRONIC COMPONENTS AND VARIABLE LATTICE SPECIFIC HEAT

When a strong shock wave propagates in a porous metal, the latter acquires sufficient energy to turn into a liquid or even a high-pressure gas. We know that the specific heat of the liquid, due to the thermal motion of the atoms at temperatures close to the melting point, is close to 3R and tends with rising temperature to the value 3R/2 characteristic of gases.[9] Similarly, $\lambda_l \to 2/3$. It is also known that an increase in density is equivalent to a decrease in temperature. Consequently, the temperatures at which the specific heat begins to deviate noticeably from 3R increase with increasing density of the substance.

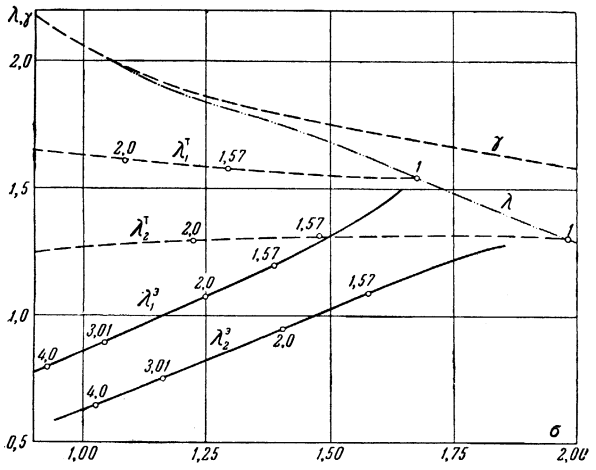

FIG. 7. Variation of λ with density for copper: along the "equal charge line" of Fig. 2 – continuous lines; along the "equal charge line" of[6] – dashed lines; along the dynamic adiabat with m = 1 – dash-dot lines; o – points corresponding to the given porosity.

The foregoing conditions can be related by the following interpolation equations*:

$$P_{T1} = \frac{3\gamma + z}{1+z}\rho R(T - \hat{T}), \tag{6}$$

$$E_{T1} = \frac{2+z}{1+z}\cdot\frac{3}{2}R(T - \hat{T}), \tag{7}$$

$$C_v = \tfrac{3}{2}R[1 + (1+z)^{-2}], \tag{8}$$

$$\lambda_1 = 2(3\gamma + z)/3(2+z). \tag{9}$$

In (6)—(9), the Grüneisen coefficient γ is related with c_c [see Slater and Landau[13, 14]] by

$$\gamma = {}^1/_3 + d\ln c_c / d\ln\rho, \tag{10}$$

and $z = lRT/c_c^2$, where l is an experimentally determined constant.

It is easily seen that as $z \to 0$ Eqs. (6) and (7) reduce to the known Mie-Grüneisen equation of state

$$P - P_c = \gamma\rho(E - E_c), \qquad C_v = 3R, \qquad \lambda_1 = \gamma; \tag{11}$$

and in the other limiting case, as $z \to \infty$, we have

$$P = \rho RT, \qquad C_v = {}^3/_2 R, \qquad \lambda_1 = {}^2/_3.$$

For finite values of z, the joint effect of the temperature and density (via c_c) is contained in z itself. The intrinsic compatibility of Eqs. (6) and (7) follows from the fact that they can be derived from the expression for the free energy of the crystal, supplemented by a term of the form $F = 3RT\ln(1+z)^{1/2}$.*

Let us turn to the thermal electronic components of the pressure, P_{T_e}, and of the energy, E_{T_e}, which play an appreciable role in the compression in the temperature ranges considered. The fully satisfactory Thomas-Fermi description[16, 17] of the experimental values of the coefficient of electronic specific heat β of simple metals at $T \sim 0°K$, enables us to employ this model to determine the dependence of β on T. For temperatures on the order of $(30—50) \times 10^3$ deg K, we can write for the thermal energy of the electrons $E_{T_e} = \beta(\rho)T^2/2$.[4,6] At higher temperatures, however, lifting of the electron-gas degeneracy begins, and the denser the substance the higher the degeneracy temperature.

The joint effect of temperature and density was calculated by Latter[17] who solved the Thomas-Fermi equation for $T \neq 0$. We shall approximate his data by the relation

$$E_{Te} = (b^2/\beta)\ln\mathrm{ch}(\beta T/b), \tag{12}$$†

which yields $E_{T_e} = \beta T^2/2$ when $T \ll b/\beta$, and which at finite T can be reconciled with Latter's results[17] by varying the parameter b (up to temperatures for which $2E_{T_e}/\beta T^2 \geq 0.5$). The thermal pressure of the electrons is given by the expression‡

$$P_{Te} = g\rho E_{Te} = g\rho(b^2/\beta)\ln\mathrm{ch}(\beta T/b), \qquad g = -d\ln\beta/d\ln\rho. \tag{13}$$

Adding (6) to (13) and (7) to (12) and taking the elastic ('cold') components into account, we write down the resultant equation of state for metals in the form

$$P = P_c(\rho) + \frac{3\gamma(\rho) + z(\rho, T)}{1 + z(\rho, T)}\rho R(T - \hat{T}) + g(\rho)\rho\frac{b^2}{\beta(\rho)}\ln\mathrm{ch}\frac{\beta(\rho)T}{b}, \tag{14}$$

*Equation (8) is valid when $T \ll \hat{T}$.

*According to Dugdale and McDonald[15] the frequency of oscillation of the atoms in a solid is determined by the isothermal speed of sound when $T \sim 0°K$ and by the isentropic speed of sound at $T \sim 300°K$ and above. V. P. Kopyshev (private communication) has shown that the limiting transition to a perfect gas can be obtained by writing down the frequency in the expression for the free energy of the crystal in the form $\omega \approx \rho^{1/3} \times (dP/d\rho)_T$. This relation, however, leads to a differential equation that has no analytic solution.

†ch = cosh

‡Relations (12) and (13) must be substituted for P_{T_e} and E_{T_e} in (3) and (4) whenever $T \geq T_{cr} = (12b^2\Delta P_{T_e}/g\rho\beta^3)^{1/4}$, where ΔP_{T_e} is the permissible error in pressure, which is known to stay within the experimental scatter. For copper, for example, when $\sigma = 1$ and $\Delta P_{T_e} = 10^{11}$ dyn/cm², we have $T_{cr} \sim 7 \times 10^4$ deg K.

$$E = E_c(\rho) + \frac{2 + z(\rho, T)}{1 + z(\rho, T)} \cdot \frac{3}{2} R(T - \hat{T}) + \frac{b^2}{\beta(\rho)} \ln \operatorname{ch} \frac{\beta(\rho) T}{b}. \quad (15)$$

The Mie-Grüneisen equation of state (11) and the equation of state with electronic components [(3) and (4)] (see also [4,6]) are particular cases of (14) and (15). The conclusions derived in the introduction regarding the possible forms of shock adiabats hold also for this equation of state.

4. RESULTS OF EXPERIMENTAL DATA REDUCTION

In the reduction of the experimental data we assumed that we know the coefficient of electronic specific heat β_k at $T \sim 0°K$ and $\rho = \rho_k$ (from measurements made at temperatures close 0°K), and the coefficient b which determines the function $E_{T_e}(T)$. Under these assumptions (see [4,6] for the motivation) the unknown parameters in the equation of states are $P_c(\rho)$, g, and l (which is included in z). The connection between γ and P_c is given by (10), with

$$c_c^2 = \frac{dP_c}{d\rho}, \qquad E_c = \int_{\rho_k}^{\rho} P_c \frac{d\rho}{\rho^2}.$$

We shall show that at compressions up to $\sigma \leq 1.5$–1.7, $P_c(\rho)$ is determined with sufficient reliability from the dynamic adiabat of the nonporous substance (for example, by the method de-

Table III

Metal	ρ_0, g/cm³	ρ_k, g/cm³	$P_{H1}\cdot10^{-12}$, dyn/cm²	$P_{H2}\cdot10^{-12}$, dyn/cm²	m_1	m_2	γ_0	$c_c\cdot10^{-5}$, cm/sec	β_k, erg/g-deg²	$b\cdot10^{6}$, erg/g-deg
Al	2.71	2.746	0.71	—	2.98	—	2.13	5.21	518	33
Cu	8.93	9.024	1.46	3.42	3.36	4.18	2.06	3.93	109	12
Pb	11.34	11.605	—	—	—	—	2.72	1.93	144	8
Ni	8.9	8.966	1.80	4.96	2.72	2.78	2.12	4.58	1240	106

Table IV

Metal	l	g	a_i, 10^{-12} dyn/cm²						
			a_1	a_2	a_3	a_4	a_5	a_6	a_7
Al	6	0.5	—0.1621	1.9795	—4.3520	—1.9795	8.2918	—4.5069	0.7292
Cu	9	0.5	14.3984	—131.0214	366.3457	—477.1198	315.2393	—100.1092	12.2670
Pb	30	0.8	0.0727	—2.2235	12.5972	—26.5633	23.5645	—8.5852	1.1376
Ni	10	1.0	18.6583	—173.8799	500.3444	—673.9271	463.1880	—154.3332	19.9495

Table V

δ	$P_c\cdot10^{-10}$, dyn/cm²	$c_c^2\cdot10^{-10}$, cm²/sec²	γ	$E_c\cdot10^{-10}$, erg/g	$P_c\cdot10^{-10}$, dyn/cm²	$c_c^2\cdot10^{-10}$, cm²/sec²	γ	$E_c\cdot10^{-10}$, erg/g
	Copper				Nickel			
1.1	17.1	22.03	1.987	0.0778	23.0	30.03	2.013	0.1061
1.2	40.1	29.22	1.927	0.3103	54.3	39.93	1.930	0.4227
1.3	70.1	37.54	1.872	0.6945	95.1	51.27	1.858	0.9468
1.4	108.2	46.98	1.821	1.2302	146.6	63.98	1.797	1.6777
1.5	155.2	57.50	1.775	1.9182	210.2	78.00	1.742	2.6158
1.6	212.3	69.07	1.732	2.7598	286.9	93.25	1.693	3.7616
1.7	280.2	81.63	1.692	3.7564	377.8	109.66	1.648	5.1154
1.8	359.9	95.15	1.655	4.9090	483.8	127.15	1.607	6.6772
1.9	452.2	109.56	1.621	6.2184	606.1	145.63	1.569	8.4462
2.0	557.9	124.82	1.589	7.6852	745.2	165.02	1.535	10.422
	Lead				Aluminum			
1.1	5.9	6.15	2.265	0.0199	9.2	38.88	1.862	0.1375
1.2	14.4	8.45	2.056	0.0840	21.4	50.03	1.711	0.5484
1.3	25.7	11.00	1.913	0.1924	35.8	61.83	1.604	1.2164
1.4	40.0	13.79	1.808	0.3457	55.4	74.18	1.522	2.1285
1.5	57.7	16.80	1.726	0.5442	77.6	87.00	1.457	3.2720
1.6	79.1	20.02	1.661	0.7879	103.2	100.23	1.403	4.6348
1.7	104.3	23.44	1.607	1.0764	132.6	113.79	1.358	6.2056
1.8	133.6	27.05	1.561	1.4096	165.8	127.65	1.319	7.9737
1.9	167.1	30.82	1.522	1.7867	202.8	141.74	1.285	9.929
2.0	205.2	34.75	1.487	2.2072	243.6	156.03	1.254	12.061
2.1	247.9	38.84	1.457	2.6704	288.5	170.46	1.227	14.362
2.2	295.4	43.06	1.429	3.1755	337.3	185.02	1.201	16.822
2.3	347.8	47.42	1.404	3.7218	390.1	199.65	1.178	19.434

veloped in [6]) subject to the assumption that $l = 0$ and $g = 0.5$. Knowing $P_c(\rho)$, we can determine $g(l)$ for each experimental point from the shock compression of the porous metal, and obtain the values of g and l, which are assumed constant. This method was used to find g and l for aluminum, porous specimens of which were investigated only under equal-charge conditions.

Having obtained experimental data for two pressures at the same density (Cu, Ni, Pb, see Figs. 4, 5, and 6), we can also determine g and l within the investigated density interval, without assuming g to be independent of the density (l remains constant as before). The parameters g and l are determined most reliably for $\sigma \approx 1$, when P_c and E_c are close to zero, and γ and c_c are known from the properties of the substance under normal conditions. In this case there is no need to make any assumptions whatever concerning the functions $\gamma(\rho)$ and $\beta(\rho)$.* This method was used for copper and nickel.

For nickel, using the limiting density $\sigma_{lim} \sim 1$ experimentally found for the adiabat with $m = 3$, we can obtain g from (5)† and l from the point with $P_H = 1.64 \times 10^{12}$ dyn/cm^2 and $\sigma = 0.941$, where the thermal pressure of the lattice amounts to about 50% of the total pressure.

Table III lists the initial data, including the pressures P_{H_1} and P_{H_2} for $\sigma = 1$ on the adiabats of metals with porosities m_1 and m_2 respectively, obtained from the average data of Fig. 2. An analysis of the behavior of $g(l)$ shows that for simple metals (aluminum, copper) the parameter l cannot be equal or close to zero, for it would lead to $g < 0$, which is obviously impossible in the investigated temperature range.‡ The obtained values of g and l are given in Table IV. They are accurate to ± 10%, taking the experimental scatter into account. It is characteristic that a value $g = 0.46$ has been obtained for porous copper metal at $\sigma = 1$, which is close to the value that follows from the Thomas-Fermi model [16,17] ($g = 0.55$), while the value obtained for the transition metal nickel is approximately twice the corresponding Thomas-Fermi value. The values of $P_c(\rho)$ were recalculated by the method described in [16,20] within the framework of the equation of state given by (14) and (15), with g and l taken from Table IV. These values were specified in the form

$$P_c = \sum_{i=1}^{7} a_i \delta^{i/3+1}, \qquad (16)$$

where $\delta = \rho/\rho_k$, and ρ_k is the density of the substance at P = 0 and T = 0°K. The reference points were chosen on the dynamic adiabats of the nonporous metals, since they come closest to $P_c(\delta)$. The values obtained are listed in Table IV,* while P_c, E_c, c_c^2 and γ are listed in Table 5.

Calculations have shown that the $P_c(\delta)$ curves coalesce smoothly with the TFC curves obtained by Kalitkin with the aid of the statistical Thomas-Fermi model with quantum and exchange corrections,[21] for $P \sim 10^{14}$—10^{15} dyn/cm^2, without crossing these curves anywhere. The parameters obtained from (2), (13), and (15) were used to calculate the shock adiabats of metals with different initial porosity, including $m = 1$. These are represented in Figs. 3—6 by the continuous curves. It is seen from the figure that all the available experimental data, both ours and those from earlier papers [1,4,5], are in satisfactory agreement over a wide range of densities and temperatures.† A certain disparity between the calculated adiabats and individual experimental points for aluminum and copper may be due either to possible inaccuracies in the experiment or to deficiencies in the equation of state, say failure to account for the details of the transition from the solid to the gaseous state.

In the case of nickel, the obtained equation of state does not fit the point with $P_H \sim 6.9 \times 10^{12}$

*Zharkov and Kalinin[18] evaluated g from the dynamic adiabat of non-porous iron, which was determined to pressures 5×10^{12} dyn/cm^2. This method cannot yield data of any reliability, since g is evaluated in the temperature region where the electronic components still play a slight role, particularly since extrapolation of the elastic-compression curve $P_c(\rho)$ is employed here. The unrealistically large values of g which they obtained have led to adiabats of the second type with sign-reversing $(\partial P/\partial\sigma)_H$ in the vicinity of $\sigma > 1$, and resulted in an unsuccessful description of the behavior of porous iron. The latter, as well as the reversal in the sign of $(\partial P/\partial\sigma)_H$, was erroneously attributed by Zharkov and Kalinin to the fact that the temperatures attained in the experiments approached the degeneracy temperature.

†The value of g obtained from (5) without allowance for the temperature dependence of β is not more than 3% in error.

‡Concerning the possibility of $g < 0$ when $T \approx 0$°K see[19].

*The initial values of γ_0 and ρ_0 needed to find the coefficients a_i (see[6,20]) are listed in Table III; λ and K_0 were obtained from[20], P_{TFC} and P'_{TFC} were taken from[21], for a value of δ such that $(P_{TF} - P_{TFC})/P_{TF} < 0.25$—0.3.

†The dash-dot line in Fig. 3 represents the adiabat of aluminum (m = 2.08), calculated using $\gamma(\sigma)$ from[4] (also shown dash-dotted in Fig. 3) with $l = 6$ and $g = 0.5$. As can be seen from the figure, the "wave-like" form of γ from[4] leads to noticeable deviation of the adiabat from the experimental point. By decreasing l it is possible to get agreement with experiment at $\sigma \approx 1.2$, but this leads to a contradiction when $\sigma \sim 1$. The example of aluminum shows that a wave-like character of $\gamma(\sigma)$, as obtained in[1,4,5], is not descriptive of the physics of the phenomenon (a fact already noted in [6]), but is due to the data-reduction methods used in these investigations.

dyn/cm^2 and $\sigma \sim 1.3$. A somewhat better fit of all the experimental data on nickel is obtained by assuming that g depends on the density ($g = \frac{2}{3} - 9.55\delta^{-1} + 37.37\delta^{-2} - 44.05\delta^{-3} + 16.6\delta^{-4}$) and has a maximum at $\sigma = 1.3$ ($g = 1.2$). The dynamic adiabats calculated with this $g(\delta)$ and with the values P_c and γ from Table V are represented by a dash-dot line in Fig. 6.

In the case of lead, we have already noted earlier [6] its anomalous behavior under shock compression at pressures exceeding 1.5 or 2×10^{12} dyn/cm^2. Calculations show that allowance for the temperature dependence of C_V and λ_l alone cannot explain this anomaly. Only the combined effect of the high value $l = 30$ with $g = 0.8$,* which follows from the experimental adiabat with $m = 1.67$, enables us to describe all the experimental data within the limits of their scatter (see Fig. 5). What is striking is the high value of the coefficient l, which should lead to a noticeable reduction in the specific heat even at normal pressures and at temperatures above the melting point, particularly in view of the low speed of sound in lead. Such an effect was observed long ago for liquid lead [22].

The calculations show that the form obtained for the equation of state with empirically determined parameters describes fairly accurately the different thermodynamic processes over a wide range of densities, pressures, and temperatures. Thus, for copper, the maximum attained densities and pressures are respectively $\rho \sim 18$ g/cm^3 and $P_H \sim 9 \times 10^{12}$ dyn/cm^2, while the maximum attained temperature (at $\rho \sim 9.0$ g/cm^3) is 90×10^3 deg.

The increase in the internal energy during shock compression of copper and nickel of varying initial porosity is illustrated in Figs. 8 and 9. The continuous lines show the states on the dynamic adiabats of metals with $m = 1$, while the dash and dash-dot lines show respectively the states realized in the first and second groups of experiments (see Sec. 1) on porous metals. The contribution of each energy component (E_c, E_{T_l}, E_{T_e}) is shown separately. It is possible to discern a functional dependence of the pressure and energy components on the density and on the temperature because the experimental data cover different ranges, in which the contribution from each of the components predominates. The maximum thermal-energy transfer from the atoms to the lattice, E_{T_l}, exceeds the binding energy by approximately four times. It is

*It is rather interesting that lead which is usually considered a simple metal has a value of g close to the value for nickel, a transition metal.

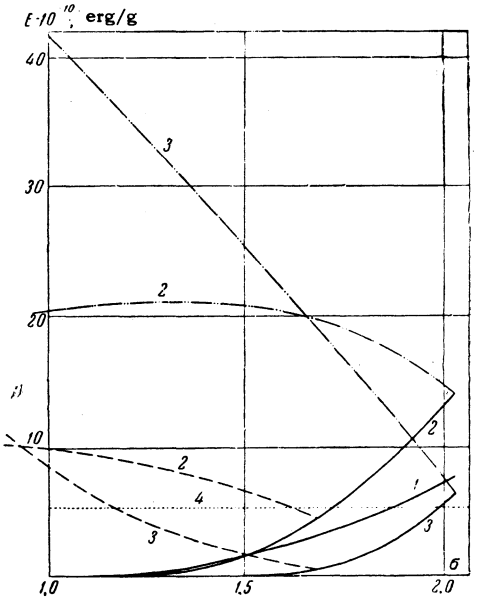

FIG. 8. Variation of the energy components with density for copper. Curve 1 – E_c, curve 2 – E_{T_l}, curve 3 – E_{T_e}, curve 4 – binding energy (heat of sublimation) for normal conditions (shown for comparison).

therefore natural for the lattice specific heat C_V to be close to 3R/2 on the boundary of the experimentally investigated region. This is illustrated in Fig. 10, where $C_V(T)$ is plotted for the four investigated metals at $\rho = \rho_k$ and $\rho = 2\rho_k$. These were calculated from (8) with experimentally obtained parameters of the equation of state. The thicker parts of the lines represent the experimentally investigated temperature interval.

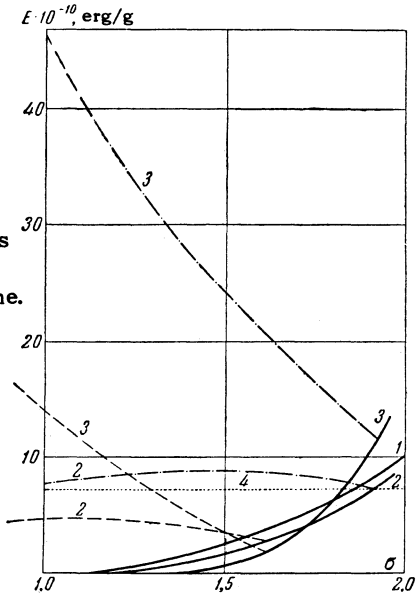

FIG. 9. The same as Fig. 8, but for nickel. The notation is the same.

In conclusion, let us determine the region where the temperature variation of C_V and λ_l must be taken into account. Figure 11 shows plots of $z(\sigma)$ for copper and nickel along the shock-

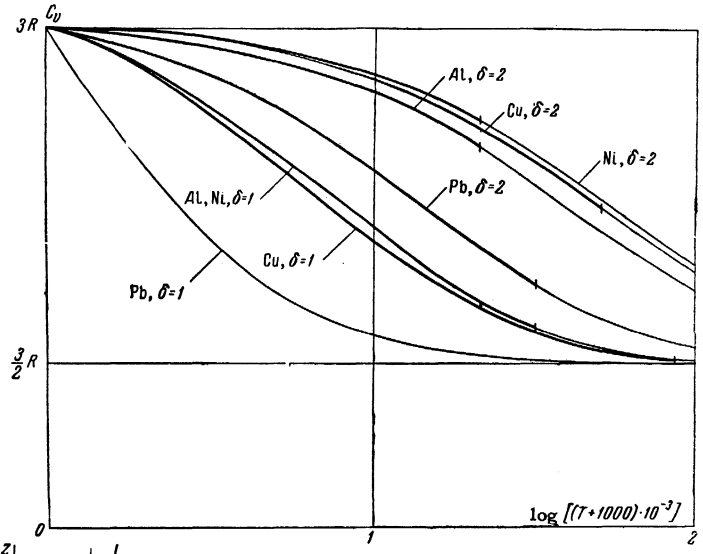

FIG. 11. Characteristics of the degree of deviation from solid-state properties on the dynamic adiabats of copper and nickel of different porosity. Solid curves – for copper, dash-dot – for nickel.

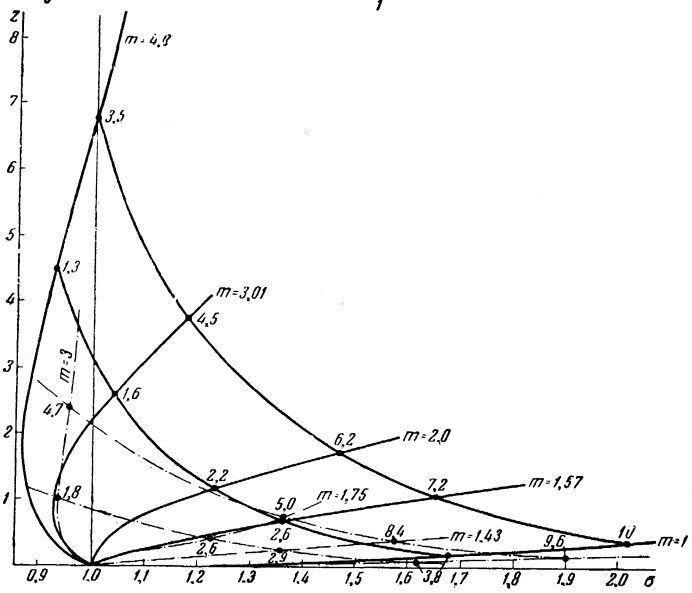

FIG. 10. Temperature variation of the lattice specific heat.

compression adiabats of solid and porous metals, and along the "equal charge lines" plotted from the obtained equations of state. The numbers along the curves indicate the pressures in 10^{12} dyn/cm^2, for which the given states are realized. It follows from the figure, for example, that for solid copper at $P_H \sim 9 \times 10^{12}$ dyn/cm^2 the deviation from the properties of a solid is less than in shock compression of a porous substance by much lower pressures. The reason is that the temperature on the front of the shock wave is much higher in porous substances than in solid ones, and is attained in the region of small compressions, where the frequency of the elastic oscillations is much less.* Starting with $z \sim 0.2$, however, it is already necessary to take the temperature dependence of C_V and λl into account on the shock-compression adiabats of the solid substances.* At the same time, analysis shows that at the prevailing accuracy of experiments on shock compression, deviations from the laws governing the theory of small oscillations [13, 14] can be noted only for $z \geq 0.5$. This means that over the entire range of pressures investigated to date, up to 10^{13} dyn/cm^2, these deviations cannot be determined from the dynamic adiabats of the solid metals alone.

Summarizing, we note that an investigation of the shock compression of porous metals enabled us to disclose deviations from the laws governing the theory of small oscillations and to arrive at

*The temperatures can be obtained from the data of Table V and from Eqs. (2), (14), and (15). For copper and nickel they can be determined from Fig. 10, using the values of l and c_c^2 from Tables IV and V. Individual isotherms are shown in Figs. 3–6.

*In the previously published papers,[4,6] where experimental data on shock-compression pressures of 2×10^{12} dyn/cm^2 for solid aluminum and 4×10^{12} dyn/cm^2 for solid copper and lead were considered, it was legitimate to disregard the temperature dependence, since $z < 0.2$ in those cases.

an equation of state in a form that describes satisfactorily the solid and liquid states of metals under high pressures and gives the correct limiting transition to the thermal pressure and the lattice energy of the gas. The form obtained for the equation of state includes, as particular cases, the equation of state with electronic components [4,6] and the Mie-Grüneisen equation of state. The experimental data obtained enabled us to find the empirical parameter l, which is used to determine the dependence of the specific heat and the ratio of the thermal pressure to the thermal-energy density of the lattice on the temperature. We also determined the electronic analog of the Grüneisen coefficient for copper and nickel, and estimated the value of this coefficient for lead and aluminum. For a simple metal such as copper it is close to that calculated by the Thomas-Fermi metal, and for the neighboring transition metal, nickel, it is approximately twice the calculated value.

The authors take this opportunity to express their deep gratitude to S. V. Ezhkov, G. M. Esin, and V. I. Efremov, who collaborated in the numerous and complicated experiments, and also to Yu. A. Glagoleva and L. T. Popova for help with the laborious calculations and the programming. The authors are most grateful to L. V. Al'tshuler, A. A. Bakanova, and R. F. Trunin for a discussion of many experimental data on shock compression of solid metals, and to K. K. Krupnikov for reporting his experimental results on porous tungsten. The authors note with special gratitude the valuable discussions and consultations with Ya. B. Zel'dovich, V. P. Kopyshev, Yu. P. Raĭzer, and K. A. Semendyaev.

[1] Walsh, Rice, McQueen, and Yarger, Phys. Rev. **108**, 196 (1957).

[2] Al'tshuler, Krupnikov, Ledenev, Zhuchikhin, and Brazhnik, JETP **34**, 874 (1958), Soviet Phys. JETP **7**, 606 (1958).

[3] Al'tshuler, Krupnikov, and Brazhnik, JETP **34**, 886 (1958), Soviet Phys. JETP **7**, 614 (1958).

[4] Al'tshuler, Kormer, Bakanova, and Trunin, JETP **38**, 790 (1960), Soviet Phys. JETP **11**, 573 (1960).

[5] R. G. McQueen and S. P. Marsh, J. Appl. Phys. **31**, 1253 (1960).

[6] Kormer, Urlin, and Popova, FTT **3**, 2131 (1961), Soviet Phys. Solid State 3, 1547 (1962).

[7] Ya. B. Zel'dovich, JETP **32**, 1577 (1957), Soviet Phys. JETP **5**, 1103 (1957).

[8] G. Ya. Galin, DAN SSSR **119**, 1106 (1958), Soviet Phys. Doklady **3**, 244 (1958).

[9] I. I. Frenkel, Kinetic Theory of Liquids, Clarendon Press, Oxford, 1946.

[10] V. V. Tovarov, Zavodskaya laboratoriya (Plant Laboratory), No. 1, 1948.

[11] Al'tshuler, Kormer, Brazhnik, Vladimirov, Speranskaya, and Funtikov, JETP **38**, 1061 (1960), Soviet Phys. JETP **11**, 766 (1960).

[12] A. G. Worthing and J. Geffner, Treatment of Experimental Data, Wiley, N. Y. 1954.

[13] J. C. Slater, Introduction to Chemical Physics, McGraw-Hill Book Company, NY. (1939).

[14] L. D. Landau and K. P. Stanyukovich, DAN SSSR **46**, 399 (1945).

[15] J. S. Dugdale and D. K. McDonald, Phys. Rev. **89**, 832 (1953).

[16] J. J. Gilvarry, Phys. Rev. **96**, 934 (1954), J. J. Gilvarry and G. H. Peebles, Phys. Rev. **99**, 550 (1955).

[17] R. Latter, Phys. Rev. **99**, 1854 (1955).

[18] V. N. Zharkov and V. A. Kalinin, DAN SSSR **135**, 811 (1960), Soviet Phys. Doklady **5**, 1253 (1961).

[19] I. M. Lifshitz, JETP **38**, 1569 (1960), Soviet Phys. JETP **11**, 1130 (1960).

[20] S. B. Kormer and V. D. Urlin, DAN SSSR **131**, 542 (1960), Soviet Phys. JETP Doklady **5**, 317 (1960).

[21] N. N. Kalitkin, JETP **38**, 1534 (1960), Soviet Phys. JETP **11**, 1106 (1960).

[22] Handbook of Chemistry and Physics, 37th Ed., Chemical Rubber Publishing Co., Cleveland, 1955—1956.

Translated by J. G. Adashko
110